

## Classification Human Brain Images and Detection Suspicious Abnormal Area

Ata'a A. Hasan<sup>1</sup>, Dr. Dhia A. Jumaa<sup>2</sup>

<sup>1</sup>(Physics, Science / Mustansiriyah University, Iraq)

<sup>2</sup>(Computer, Science / Mustansiriyah University, Iraq)

---

**Abstract:** Magnetic Resonance Images (MRI) are widely utilized in the diagnosis of brain images. In this study we have developed a new approach for automatic classification of the normal and abnormal MRI images. The proposed method consists of four stages namely preprocessing, transformation, texture feature extraction and classification. The first stage is preprocessing image and utilized filter is applied for noise reduction and to make the image suitable for transformation. In the second stage, is utilized Discrete Multiwavelet Transform (DMWT) to reduce the dimensionality. In the third stage, features extraction based combined between first order statics (FOS) and second order statics (SOS). The fourth stage in the classification stage, a supervised probabilistic neural network (PNN) classifier is utilized to classify the experimental images into normal and abnormal. Finally, proposed algorithm is to segmenting, hexagonal superpixel algorithm. The basic idea in this proposed algorithm is how to detection suspicious abnormal (tumor) area brain to reduce computational time for clinical high diagnostic. It was found this algorithm was very efficient segmentation image, which can be very powerful in the biomedical field of tumor classification.

**Keywords:** DMWT, Feature Extraction, PNN, Superpixel.

---

### I. Introduction

Brain tumor is body created of many cells. Each cell has specific duty. The cells grow in the body and are divided to reproduce other cells. These divisions are very vital for correct functions of the body. When each cell loses the capability of controlling its growth, these divisions are done without any limitations, and tumor originates [1]. Brain is the kernel part of the body. Brain has a very complex structure. And the brain can be affected by a problem which reasons change in its normal structure and its normal behavior. This problem is known as brain tumor. It is one of the main reasons for the increase in death rate among kids and adults [2]. The Brain tumors can be classified as follows [3,4]:

#### 1. Benign Brain Tumor: (Non-Cancerous Tumor)

This type of tumor usually does not include cancer cells and can be removed. Benign brain tumors generally have clear border or edge. They don't spread to other parts of the body. However, benign tumors can cause serious health problems [3].

#### 2. Malignant Brain Tumor: (Cancerous Tumor)

This includes cancer cells and therefor also named as brain cancer. They are likely to grow quickly and can affect nearby healthy brain tissues. This type of tumor can be a threat for life. It is classified as primary and secondary tumor [3,4].

##### a. Primary Tumors:

A primary tumor indicates to a tumor or mass that is growing in the location where cancer emerged. Most of them are usually easily treated with techniques such as surgery.

##### b. Secondary Tumor (Metastatic):

A secondary (Metastatic) brain tumor happens when cancer cells spread to the brain from a primary cancer in other part of the body. Secondary tumors are about three times more generally than primary tumors of the brain.

The modalities usually utilized to acquire medical images are X-rays, Computed Tomography (CT), Magnetic Resonance Imaging (MRI) and ultrasound imaging. In medical imaging, MRI is one of the scanning tackle which utilizes magnetic fields to capture images in films [5]. Compared to all other imaging techniques, MRI is active in the application of brain tumor disclosure and identification, due to the high contrast of smooth tissues, high spatial resolution and since it does not produce any harmful radiation, and is a non-invasive technique [6].

**II. Theoretical Aspect of Multiwavelet**

Wavelet theory is based on the concept of multi-resolution analysis (MRA), in which the criterion multi-resolution has one scaling function  $\phi(t)$ . However, one can imagine a core general MRA setting when several scaling functions are allowed, this concept to the notion of multiwavelet, which has several benefits in comparison to scalar wavelets. Such features as short support, orthogonality, symmetry, and vanishing moments are known to be significant in signal processing. A scalar wavelet cannot possess all these characteristics at the same time. On the other hand, a multiwavelet system can simultaneously give perfect reconstruction while preserving length (orthogonality), good performance at the boundaries (via linear-phase symmetry), and a high order of approximation (vanishing moments). Thus multiwavelets offer the possibility of superior performance for image processing applications, compared with scalar wavelets [7,8,9].

Multiwavelets are very similar to wavelets but have some significant differences. In particular, whereas wavelets have associated scaling function  $\phi(t)$  and wavelet function  $\psi(t)$ , multiwavelets have two or more scaling and wavelet functions [10]. For notational convenience, the set of scaling functions can be written using the vector notation as [11]:

$$\phi(t) \equiv [\phi_1(t)\phi_2(t) \dots \dots \dots \phi_r(t)]^T \dots \dots \dots (1)$$

where  $\phi(t)$  is named the multi-scaling functions. Similarly, the multiwavelet function is defined from the set of wavelet functions as:

$$\psi(t) \equiv [\psi_1(t)\psi_2(t) \dots \dots \dots \psi_r(t)]^T \dots \dots \dots (2)$$

When  $r = 1$ ,  $\psi(t)$  is named a scalar wavelet, or simply wavelet. While in principle  $r$  can be arbitrarily large [11,12,13].

The multiwavelet two-scale ( $r = 2$ ) equations resemble those for scalar wavelets [11,14]:

$$\phi(t) = \sqrt{2} \sum_{k=0}^{m-1} G_k \phi(2t - k) \dots \dots \dots (3)$$

$$\psi(t) = \sqrt{2} \sum_{k=0}^{m-1} H_k \psi(2t - k) \dots \dots \dots (4)$$

Note, that  $G_k$  and  $H_k$  (are matrix filters (low-pass filter and high-pass filter consecutively); i.e.,  $G_k$  and  $H_k$  are  $r \times r$  matrices for integer  $k$ , and  $m$  is number of support. The matrix elements in these filters give more degrees of freedom than a traditional scalar wavelet. These extra degrees of freedom can be utilized to incorporate useful properties into the multiwavelet filter, such as orthogonality, symmetry, and high order of approximation [13,15,16]. The multiwavelet basis utilizes translations and dilations of  $r \geq 2$  scaling functions and  $r$  mother wavelet as shown in equations (3,4) [17]. The two-scale equations (3,4) can be realized as a matrix filter bank operating on  $r$  input data streams and filtering them into  $2r$  output data streams, each of which is down sampled by a factor of two [18]. The 2-D prefiltering is performed successively to the rows and columns of the input signal resulting in four frequency subsignals. Choice of Multi-filters in practice multiscaling and wavelet functions often have multiplicity  $r = 2$ . A significant paradigm was constructed by Geronimo, Hardin, and Massopust (GHM). The GHM system contains the two scaling functions  $\phi_1(t), \phi_2(t)$  and two wavelets  $\psi_1(t), \psi_2(t)$ . The dilation and translation equations for this system have four coefficients follows [19].

$$\varphi(t) = \begin{bmatrix} \phi_1(t) \\ \phi_2(t) \end{bmatrix} = G_0 \varphi(2t) + G_1 \varphi(2t - 1) + G_2 \varphi(2t - 2) + G_3 \varphi(2t - 3) \dots (5)$$

$$G_0 = \begin{bmatrix} 3 & 4 \\ 5\sqrt{2} & 5 \\ -1 & -3 \\ 20 & 10\sqrt{2} \end{bmatrix} \quad G_1 = \begin{bmatrix} 3 & 0 \\ 5\sqrt{2} & 9 \\ 20 & 1 \\ \sqrt{2} & \end{bmatrix}$$

$$G_2 = \begin{bmatrix} 0 & 0 \\ 9 & -3 \\ 20 & 10\sqrt{2} \end{bmatrix} \quad G_3 = \begin{bmatrix} 0 & 0 \\ -1 & 0 \\ 20 & 0 \end{bmatrix}$$

And four wavelet matrices  $H_0, H_1, H_2,$  and  $H_3$

$$\psi(t) = \begin{bmatrix} \psi_1(t) \\ \psi_2(t) \end{bmatrix} = H_0 \psi(2t) + H_1 \psi(2t - 1) + H_2 \psi(2t - 2) + H_3 \psi(2t - 3) \dots (6)$$

$$H_0 = \begin{bmatrix} -1 & -3 \\ 2 & \sqrt{2} \\ 1 & 3 \\ \sqrt{2} & \end{bmatrix} \quad H_1 = \begin{bmatrix} 9 & -10 \\ 2 & \sqrt{2} \\ -9 & 0 \\ \sqrt{2} & \end{bmatrix}$$

### III. Probabilistic Neural Network

Probabilistic neural networks (PNN) are a kind of radial basis network suitable for classification problems. A PNN is primarily a classifier since it can map any input pattern to a number of classifications that is Probabilistic neural networks can be utilized for classification problems. When an input is presented, the first layer computes distances from the input vector to the training input vectors and produces a vector whose elements indicate how close the input is to a training input. The second layer sums these contributions for each class of inputs to produce as its net output a vector of probabilities. Finally, compete transfer function on the output of the second layer picks the maximum of these probabilities. PNN is a fast training process and an inherently parallel structure that is guaranteed to converge to an optimal classifier as the size of the representative training set increases and training samples can be added or removed without extensive retraining [20].

### IV. Proposed System

This work presents the proposed system started by presenting general block diagram of the natural and tumors type classification system. The proposed system is suggested to be utilized as a tool for the radiologist and surgeon. This tool is to classify normal and tumors in MRI brain images and detection suspicious abnormal area (tumor). Shown in Fig.1.

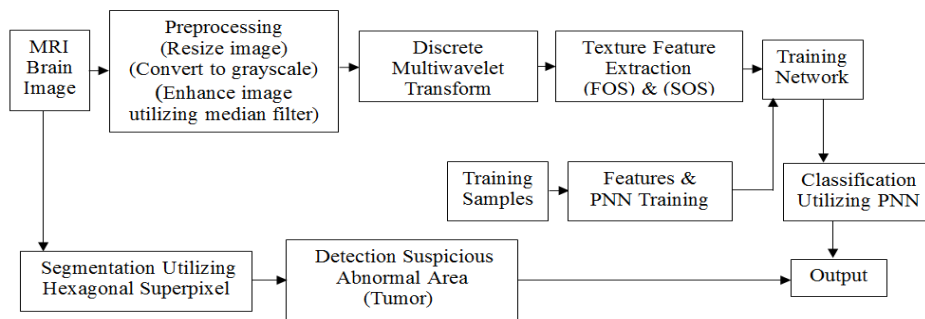


Fig.1: Block Diagram of the Normal and Tumors Type Classification System and Detection Suspicious Abnormal Area (Tumor).

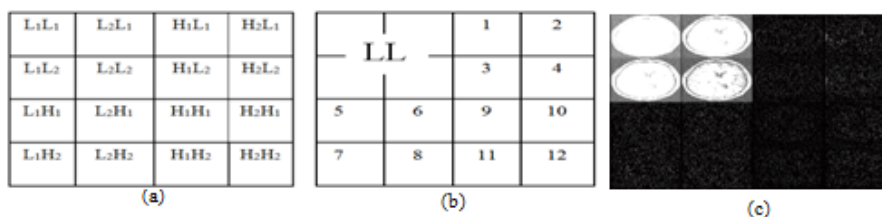
#### 4.1 First Stage (Image Perprocessing)

Image preprocessing consists mainly of following steps:

- Resize the input MRI human brain image to 256×256.
- Convert the input color image in to grayscale image utilizing RGB converter.
- Convert BMP, PNG to JPEG image (.jpg) file format.
- Apply median filter to reduce noise and to improve the quality of the input image.

#### 4.2 Second Stage (Utilizing Multiwavelet Transform)

Multiwavelet decomposition is done utilizing GHM system. The gray scale image with size (256 × 256) pixels is decomposed into one level. The result is 16 subimages, four subimages with pure low frequency features and 12 subimages with "High" features. Fig.2 represents one level decomposition and the distribution of subimages numbering.



**Fig.2:** a. One level of multiwavelet decomposition, b. Distribution of sub-images numbering, c. One Level Multiwavelet of MRI Tumor Brain Image Decomposition.

**4.3 Third Stage (Texture Feature Extraction)**

Texture feature extraction is a special form of reduction computational complexity. The simplest statistics are the gray level first-order statistics (FOS) [21]. And utilizing Second-order statistics (SOS) such as Gray-Level Co-occurrence Matrix (GLCM) proposed by Haralick [22] describes the gray level of an image. GLCM based on two pixel intensity values. The formula for calculating texture features as following [2,21]:

$$1. Mean = \mu = \sum_{i=0}^{N_g-1} i P(i) \quad \dots \dots \dots (7)$$

$$2. Average Contrast = \sigma^2 = \sum_{i=0}^{N_g-1} (i - \mu)^2 P(i) \quad \dots \dots \dots (8)$$

$$3. Energy = \sum_{i,j=0}^{N_g-1} P_d^2(i, j) \quad \dots \dots \dots (9)$$

$$4. Entropy = - \sum_{i,j=0}^{N_g-1} P_d(i, j) \log(P_d(i, j)) \quad \dots \dots \dots (10)$$

$$5. Contrast = \sum_{i,j=0}^{N_g-1} P_d(i, j) * (i - j)^2 \quad \dots \dots \dots (11)$$

$$6. Homogeneity = \sum_{i,j=0}^{N_g-1} \frac{P_d(i,j)}{1+(i,j)^2} \quad \dots \dots \dots (12)$$

$$7. Dissimilarity = \sum_{i,j=0}^{N_g-1} P_d(i, j) * |(i, j)| \quad \dots \dots \dots (13)$$

$$8. Maximum Probability = \max_{i, j} P_d(i, j) \quad \dots \dots \dots (14)$$

**4.4 Fourth Stage (Training & Testing Phases Of Pnn)**

When starting proposed system; the main interface of the system will appear on the screen, the main interface has two main phases (Training and Testing phases). The first phase in the system presented here is training and learning. In Learning/Training Phase the PNN is trained for classification of different MRI types of brain. The second phase is Classification/Testing. In this work trained the PNN with 105 images stored in database. We compute eight features extraction for eight subimages from DMWT. Hence the total feature extraction data length vector will be (105×96) for each subimages.

**Algorithm 1:** Begin

**Step1:** Read the input color medical MRI human brain images.

**Step2:** Resize the image in to 256×256 image matrix.

**Step3:** Converts the image from JPEG image (.jpg) file format to data file.

**Step4:** Converts input color image in to grayscale image.

**Step5:** Enhancement image utilizing median filter.

**Step6:** Apply the Discrete Multiwavelet Transform Decompose the image into 2-D DMWT with one level, segmentation image into 16 subimages, starting from the top left corner, (L<sub>1</sub>L<sub>1</sub>, L<sub>1</sub>L<sub>2</sub>, L<sub>2</sub>L<sub>1</sub>, L<sub>2</sub>L<sub>2</sub>, H<sub>1</sub>L<sub>1</sub>, H<sub>2</sub>L<sub>1</sub>, H<sub>1</sub>L<sub>2</sub>, H<sub>2</sub>L<sub>2</sub>, L<sub>1</sub>H<sub>1</sub>, L<sub>2</sub>H<sub>1</sub>, H<sub>1</sub>H<sub>1</sub>, H<sub>2</sub>H<sub>1</sub>, L<sub>1</sub>H<sub>2</sub>, L<sub>2</sub>H<sub>2</sub>, H<sub>1</sub>H<sub>2</sub>, and H<sub>2</sub>H<sub>2</sub>).

**Step7:** Compute the normalized for each subimages except the one with "low-low" subimage (L<sub>1</sub>L<sub>1</sub>, L<sub>1</sub>L<sub>2</sub>, L<sub>2</sub>L<sub>1</sub>, L<sub>2</sub>L<sub>2</sub>) utilizing of first order statics (FOS) mean utilizing equation (7), average contrast utilizing equation (8) and second order statics (Gray Level Co-occurrence Matrix) (CLCM) with d=1 for distance and θ = 0 degrees, energy utilizing equation (9), entropy utilizing (10), contrast utilizing equation (11), homogeneity equation (12), dissimilarity utilizing equation (13), max probability utilizing (14).

**Step8:** Save the normalized mean, average contrast, energy, entropy, homogeneity, and maximum probability in the feature extraction file DB.

**Step9:** Build the PNN and load the feature extraction data (DB) to train the neural network.

**Step10:** Input the results from steps (6 and 7) to the neural network.

**10.1** Find the estimated PDF for each hidden node in pattern layer.

**10.2** Find the sum of each node in summation layer (summation of estimated PDF for each class).

**10.3** Find the probability of each class by divided the sum of estimated PDF for each class over the sum of all estimated PDF.

**10.4** Find the reference in feature extraction file.

**Step11:** Assign the unknown image to class with probability largest.

End

**4.5 Example Of Testing Phase For Dmwt**

To improve the correctness of the algorithm, let us take an example to demonstrate the application of the recognition algorithm. The example is:

**Step1:** Read medical MRI brain image (Test-Image/.Glioblastoma multiform).

**Step2:** Resize the image in to 256×256 image matrix.

**Step3:** Converts the image from JPEG image (.jpg) file format to data file.

**Step4:** Converts input color image in to grayscale image.

**Step5:** Enhancement image utilizing median filter.

**Step6:** Decompose the image into 2-D DMWT with one level to get 16 subimages.

**Step7:** The normalized mean, average contrast, energy, entropy, contrast, homogeneity, dissimilarity, and maximum probability of the 12 subimages are:

Sub images	Contrast	Homogeneity	Dissimilarity	Energy	Entropy	Average Contrast	Mean	Maximum Probability
L <sub>1</sub> H <sub>1</sub>	3.9146	0.0145	3.0583	1.9497	3.7294	6.9000	0.0583	74.0202
L <sub>1</sub> H <sub>2</sub>	1.5359	0.0113	7.9998	6.9547	2.9791	13.0317	0.1017	112
L <sub>2</sub> H <sub>1</sub>	1.0088	0.0601	1.5763	1.2901	3.9572	5.6126	0.0601	70.4578
L <sub>2</sub> H <sub>2</sub>	6.7498	0.0251	5.2733	4.8772	3.1713	10.9129	0.1005	100
H <sub>1</sub> L <sub>1</sub>	4.2147	0.0157	3.2927	2.2629	3.6287	7.4335	0.0628	71.6936
H <sub>1</sub> L <sub>2</sub>	3.3996	0.0020	5.3120	1.4541	3.7532	5.9590	0.0020	59.4186
H <sub>1</sub> H <sub>1</sub>	5.9418	0.0760	5.3797	7.9939	3.0748	13.9551	0.6840	136
H <sub>1</sub> H <sub>2</sub>	3.7991	0.1415	2.9680	5.2152	3.2302	11.2711	0.5661	93.7436
H <sub>2</sub> L <sub>1</sub>	0	6.3099	0	6.9338	4.5562	1.3011	0.0154	18.5193
H <sub>2</sub> L <sub>2</sub>	3.0080	0.0011	2.3685	1.4017	4.3498	1.8501	0.0045	17.7338
H <sub>2</sub> H <sub>1</sub>	1.3612	0.0081	2.1269	1.2964	4.2738	1.7792	0.0081	15.0130
H <sub>2</sub> H <sub>2</sub>	0	5.1562	0	5.0091	4.2387	3.4974	0.0125	35.2766

**Step8:** Build the probabilistic Neural Network.

**Step9:** Load the training data to train the neural network.

**Step10:** Input the results from step (7) to the neural network.

**10.1:** The estimated PDF for each hidden node in pattern layer are:

0.7584	0.7552	0.7550	0.7701	0.7481	0.8913	0.7544
0.8391	0.7443	0.7444	0.7868	0.7395	0.7543	0.8139
0.7982	1.2043	0.7619	0.7976	0.7531	0.7408	0.7802
0.8071	0.7533	1.5484	0.8398	0.7622	0.7775	0.7722
0.7518	0.7685	0.7719	0.9279	0.8064	0.8399	0.7503
0.8291	0.7651	0.7498	0.7841	1.0118	0.7948	0.9976
0.7586	0.7494	0.8086	0.7640	0.8108	0.7413	0.8271
0.7491	0.7991	0.7553	0.7422	0.7493	0.7676	0.7500
0.7503	0.7761	0.7532	0.7531	1.0111	0.7411	0.7855
0.7589	0.7421	0.7638	0.7576	0.7421	0.7830	0.8077
0.7527	0.7441	0.7572	0.7664	0.7541	0.7641	0.7464
0.7551	0.8111	0.7741	0.9401	0.7581	0.7429	0.7606
0.7650	0.7469	0.7474	0.9877	0.7532	0.7635	0.8219
0.7498	0.7566	0.7685	0.8569	0.7674	0.7527	0.7411
0.7781	0.7533	0.8025	0.7488	0.7595	0.7531	0.7548

**10.2:** The summation of each node in summation layer(summation of estimated PDF for each class) are:

Sum <sub>1</sub>	Sum <sub>2</sub>	Sum <sub>3</sub>	Sum <sub>4</sub>	Sum <sub>5</sub>	Sum <sub>6</sub>	Sum <sub>7</sub>
11.8140	14.2183	12.7437	12.4634	11.6923	12.1848	11.5056

The total summation = 86.6220

**10.3:** The probability of each class by dividing the summation of estimated PDF for each class over the summation of all estimated PDF are:

P <sub>1</sub>	P <sub>2</sub>	P <sub>3</sub>	P <sub>4</sub>	P <sub>5</sub>	P <sub>6</sub>	P <sub>7</sub>
0.1364	0.1641	0.1471	0.1439	0.1350	0.1407	0.1328

**Step11:** Assign the unknown image to a class that is fired from PNN (with largest probability)  
(Class = Glioblastoma multiform)

**Step12:** End.

## V. Utilizing Super pixel Segmentation for Detection Suspicious Abnormal Area.

Supapixel provides a serviceable initial from which to compute local image features, they capture redundancy in the image, and greatly reduce the complexity of subsequent image processing tasks [23]. The fact of good pixel packing, and uniformity in size of pixels determine the performance of the proposed algorithm. The efficiency of the algorithm is measured by boundary recall and under-segmentation error measures [24]. There are many approaches to generate superpixel, each with its own advantages and drawbacks that may be better suited to a particular application [23]. Such as those generated by Simple Linear Iterative Clustering (SLIC) Superpixel in Fig.4, are desirable.

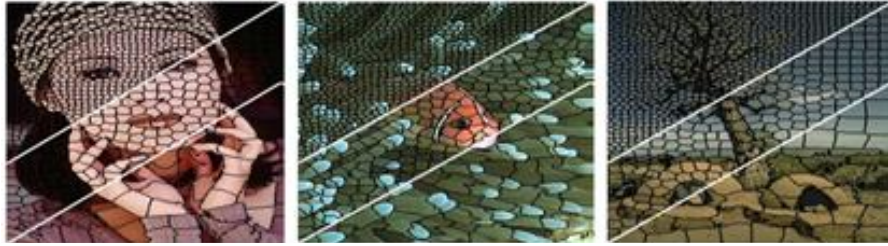


Fig.4: Images segmented utilizing SLIC into superpixel of size 64, 256, and 1, 024 pixels [24,25,26].

SLIC method for generating superpixel which is faster than existing methods, more memory efficient, exhibits state-of-the-art boundary adherence, and improves the performance of segmentation algorithms. SLIC is an adaptation of k-means clustering for superpixel generation; a weighted distance measure combines color and spatial proximity while simultaneously providing control over the size and compactness of the superpixels. The clustering is done on the five-dimensional [labxy] space, where [lab] is the pixel color vector in CIELAB color space and xy is the pixel co-ordinates. The maximum possible color distance between two nearing colors in the CIELAB space is limited and the spatial distance is determined by the image size. The spatial distance is to be normalized in order to apply the Euclidean distance in this 5D space. Hence, new distance measure that considers superpixel size by taking into account a different weighting factor[27]. Distance measure  $D_s$  is defined as:

$$d_{lab} = \sqrt{(l_j - l_i)^2 + (a_j - a_i)^2 + (b_j - b_i)^2} \quad \dots \dots \dots (16)$$

$$d_{xy} = \sqrt{(x_j - x_i)^2 + (y_j - y_i)^2} \quad \dots \dots \dots (17)$$

$$D_s = d_{lab} + \frac{m}{S} d_{xy} \quad \dots \dots \dots (18)$$

Where  $D_s$  is the sum of the lab distance and the (xy) plane distance normalized by the grid interval S. A variable m is introduced in D' allowing us to control the compactness of superpixel. The greater value of m, the more spatial proximity is emphasized and the more compact the cluster [27]. The algorithm of Hexagonal method superpixel is the main idea of this method is how to locate the initial seeds for the (n) clusters (superpixel) over the image which this is a fundamental parameter that determines the boundaries (initial state) of the spreading segments. After determining a suitable threshold value for splitting image region as well as the minimum size of the final splitting window, image will be divided multiple windows. Selecting centers of these windows will be utilized as the seeds points (seeds determine location and intensity value as well). If superpixel no. (clusters no.) is more less than the generated windows, the biggest ones will be selected as the proposed. For features no. the original image which is already a true color one is transformed into (HSV) format. The (V) layer will be utilized for segmentation in addition to the geometrical feature (distance from the seed center). Similarity criterion that was utilized for segmentation will be Euclidean distance formula. Normalized formula will be adopted in this algorithm. Splitting superpixel algorithm can be given in algorithm (2). The search space is a small square window to decrease computations time. The clusters are updated in whole iteration, based on the location and intensity distance of the pixels in search area to the centers. Therefore, the centers location is changed in every loop by calculating the gravity centers of new clusters. A seed point is selected in an arbitrary image by the utilizer. Then we determined threshold value of the hexagonal superpixel algorithm which contains this point and we checked threshold value of the neighboring hexagonal superpixels.

**Algorithm 2:** Begin

- Step1:** Read the input medical MRI brain color image.
- Step2:** Convert color image from RGB format to HSV format.
- Step3:** Select the 'V' layer to be processing.
- Step4:** Distribution (row×col) superpixel cell over image space hexagonal.
- Step5:** For each superpixel cell.
- Step6:** Open window around superpixel center.
- Step7:** Take the color of superpixel center as superpixel color.
- Step8:** If it full fill similarity value.

$$distance = \sqrt{(Superpixelx_c - pixelx)^2 + (Superpixely_c - pixely)^2}$$

$$similarity = \sqrt{w_1 \times (pixelcolor - superpixelcolor)^2 + w_2 \times distance}$$

- Step9:** If similarity <= threshold assign pixel superpixel number.
  - Step10:** Loop.
- End

## VI. Experimental Results and Discussion

In this paper, an automatic brain tumor classifier was proposed. The proposed technique was implemented on MRI dataset (these are Lymphoma, Glioblastoma multiform, Cystic oligodendroglioma, Ependymoma, Meningioma and Anaplastic astrocytoma. The numbers of collected images are 140 (20 images for each type of the six tumors and 20 image normal cases). The algorithm described in this paper is developed and successfully trained in MATLAB version R3010b utilizing a combination of image processing and neural network toolbox. The remaining 35 MRIbrain images from different types will be utilized as testing data phase. The result represents that 34 images are classified correctly and the one image are not classified correctly. The initial superpixel centers are located by uniform sampling the pixels in one image in 2D space. The search space is a small square window to decrease computations time. The clusters are updated in whole iteration, based on the location and intensity distance of the pixels in search area to the centers. Therefore, the centers location is changed in every loop by calculating the gravity centers of new clusters. A seed point is selected in an arbitrary image by the utilizer. Then we determined threshold value of the hexagonal superpixel algorithm which contains this point and we checked threshold value of the neighboring hexagonal superpixels. Fig.5 hexagonal superpixel segmentation for suspicious abnormal area.

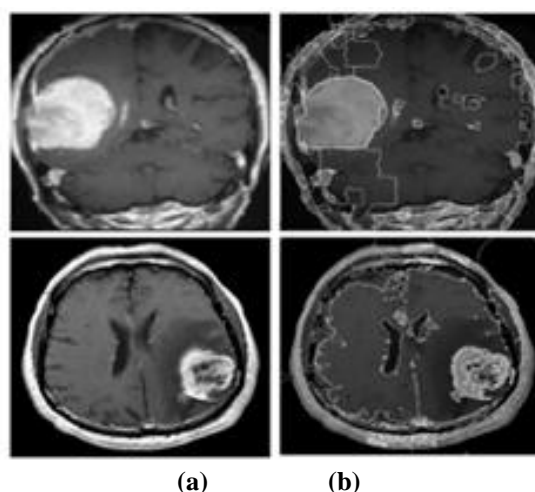


**Fig.5: a.** Original Image, **b.** Image after implementation Hexagonal Superpixel Segmentation for suspicious abnormal area Image with the following parameters ( $th_1=0.15$ ,  $th_2=0.4$ ).

## VII. Conclusions

MRI image is one of the best methods in brain tumor classification and detection, by observing only MRI images the specialists are unable to keep up with diagnosing. Hence, the computer based diagnosis is necessary for the correct brain tumor classification. The new method is a combination of Discrete Multiwavelet Transform, Texture features extracted and Probabilistic Neural Network. By utilizing this algorithm, an efficient brain tumor classification method is been constructed with maximum classification rate of 97%. The are utilized to classify the class of the tumor as normal & abnormal. And the benefit of utilizing hexagonal superpixel segmentation proposed new algorithm had be utilized to improve high accuracy diagnostics and fast application very efficient with MRI brain images due to detected suspicious abnormal area (tumor brain) image and hexagonal superpixel segmentation gives visual meaning, because gives uniform and meaningful representation of image based on texture and color.

## References

- [1] A. Lashkari, A Neural Network-Based Method for Brain Abnormality Detection in MR Images Using Zernike Moments and Geometric Moments, *International Journal of Computer Applications*, 4(7), 2010, 1-8.
- [2] Q.U. Ain, G. Latif, S.B. Kazmi, M.A.Jaffar, and A.M.Mirza, Classification and Segmentation of Brain Tumor using Texture Analysis, *proceedings of the 9th WSEAS International Conference on Artificial Intelligence, Knowledge Engineering and Databases (AIKED)*, 2010, 147-155.
- [3] G. Anandgaonkar and G. Sable, Brain Tumor Detection and Identification from T1 Post Contrast MR Images Using Cluster Based Segmentation, *International Journal of Science and Research (IJSR)*, 3(4), 2014, 814-817.
- [4] D.B.Kadam, S.S. Gade, M.D. Uplane and R.K. Prasad, Neural Network Based Brain Tumor Detection Using MR Images, *International Journal of Computer Science and Communication (IJCSC)*, 2(2), 2011, 325-331.
- [5] N. Abdullah, U.K. Ngah and S.A. Aziz, Image Classification of Brain MRI Using Support Vector Machine, *IEEE International Conference on Imaging Systems and Techniques*, 2011, 242-247.
- [6] P. John, Brain Tumor Classification Using Wavelet and Texture Based Neural Network, *International Journal of Scientific & Engineering Research*, 3(10), 2012, 1-7.

- [7] V. Strela and P.N. Heller, G. Strang, P. Topiwala and C. Heil, The Application of Multiwavelet Filter Bank to Image Processing, *IEEE Transactions on Image Processing*, 8(4), 1999, 548-563.
- [8] G. Plonka, and V. Strela, From Wavelets to Multiwavelets, *Mathematical Methods for Curves and Surfaces*, 1998, 375-399.
- [9] E.P. Kumar, and M.G. Sumithra, MEDICAL IMAGE COMPRESSION USING INTEGER MULTI WAVELETS TRANSFORM FOR TELEMEDICINE APPLICATIONS, *International Journal Of Engineering And Computer Science*, 2(5), 2013, 1663-1669.
- [10] B. Michael and E. Amy, New Image Compression Techniques Using Multi Wavelets and Multi Wavelets packet, *IEEE Transactions Image Processing*, XX(Y), 2000, 1-10.
- [11] E. Sankaralingam, V. Thangaraj, S. Vijayamani, and N. Palaniswamy, Video Compression Using Multiwavelet and Multistage Vector Quantization, *The International Arab Journal of Information Technology*, 6(4), 2009, 385-393.
- [12] H.S. Zadeh, and K. J. Khouzani, Multiwavelet Grading of Prostate Pathological Images, *IEEE Transactions on Biomedical Engineering*, 52(12), 2005, 2074-2086.
- [13] V. K. Sudha, and R. Sudhakar, MULTI WAVELET TRANSFORM IN COMPRESSION OF MEDICAL IMAGES", *ICTACT JOURNAL ON IMAGE AND VIDEO PROCESSING*, 3(4), 2013, 616-619.
- [14] K. Bao, and X.G. Xia., Image Compression Using a New Discrete Multiwavelet Transform and a New Embedded Vector Quantization, *IEEE Transaction on Circuits and Systems for Video Technology*, 10(6), 2000, 833-842.
- [15] A.A. Jumah, M.G. Ahamad, and S.A. Ali, Denoising of Medical Images Using Multiwavelet Transforms and Various Thresholding Techniques, *Journal of Signal and Information Processing*, 4, 2013, 24-32.
- [16] S. Rout and A.E. Bell, Color image compression multi wavelets vs. Scalar wavelets, *Acoustics, Speech, and Signal Processing (ICASSP), 2002 IEEE International Conference*, 4, 2002, IV-3501 - IV-3404.
- [17] I.W. Selesnick, Balanced multi wavelets bases based on symmetric FIR Filter, *IEEE TRANSACTIONS ON SIGNAL PROCESSING*, 48(1), 2000, 184-191.
- [18] V. Strela and A.T. Walden, Orthogonal and biorthogonal multiwavelets for signal denoising and image compression, *International Society for Optical Engineering*, 3391, 1998.
- [19] B.R. Johnson, Multiwavelets moments and projection prefilters, *Signal Processing, IEEE Transactions on Signal Processing*, 48(11), 2002, 3100-3108.
- [20] S. Jain and S. Mishra, ANN Approach Based On Back Propagation Network and Probabilistic Neural Network to Classify Brain Cancer, *International Journal of Innovative Technology and Exploring Engineering (IJITEE)*, 3, 2013, 101-105.
- [21] N. Nabizadeh and M. Kubat, Brain tumors detection and segmentation in MR images: Gabor wavelet vs. statistical features, *Computers and Electrical Engineering xxx (2015) xxx-xxx*, 2015, 1-15.
- [22] R. M. Haralick and K. Shanmugam, Textural feature for image classification, *IEEE Transactions on Systems, Man, And Cybernetics*, 1980, SMC-3(6):610-619.
- [23] R. Achanta, A. Shaji, K. Smith, A. Lucchi, P. Fua, and S. Ssstrunk, SLIC Superpixels Compared to State-of-the-Art Superpixel Methods, *Journal of Latex Class Files*, 6(1), 2011.
- [24] S. Ranjitham and K. Padmavathi, Superpixel Based Color Image Segmentation Techniques: A Review, *International Journal of Advanced Research in Computer Science and Software Engineering*, 4(9), 2014, 465-471.
- [25] R. Achanta, A. Shaji, K. Smith, A. Lucchi, P. Fua, and S. Ssstrunk, SLIC Superpixel, *EPFL Technical Report 149300*, 2010, 1-10.
- [26] R. Achanta, A. Shaji, K. Smith, A. Lucchi, P. Fua, and S. Ssstrunk, SLIC Superpixels Compared to State-of-the-Art Superpixel Methods, *IEEE Transactions on Pattern Analysis and Machine Intelligence*, 34(11), 2012, 2274-2282.
- [27] C.Y. Ren and I. Reid, gSLIC : a real-time implementation of SLIC superpixel segmentation, *University of Oxford, Department of Engineering Science, Parks Road, Oxford, UK*, 2011, 1-6.